FBR-TM-71-2

Wood

Rec'd from printing 20 April '71

These results plus the results generated since Dec. will eventually be incorporated into a Tech. Rpt.

Baker

AIR FORCE FLIGHT DYNAMICS LABORATORY
DIRECTOR OF LABORATORIES
AIR FORCE SYSTEMS COMMAND
WRIGHT PATTERSON AIR FORCE BASE OHIO

AF FLIGHT DYNAMICS LABORATORY

FBR 5763

Crack Propagation Test Results for Variable Amplitude Spectrum Loading in Surface Flawed D6ac Steel

prepared by

H.A. Wood
T.L. Haglage

Technical Memorandum FBR-71-2

February 1971

FBR-TM-71-2

Crack Propagation Test Results for Variable Amplitude Spectrum Loading in Surface Flawed D6ac Steel

prepared by

H.A. Wood
T.L. Haglage

Technical Memorandum FBR-71-2

February 1971

FOREWORD

This work was conducted by Mr. Howard A. Wood and Mr. Theodore L. Haglage, under the supervision of Mr. R.M. Bader, Technical Manager, Analysis Group, at the Air Force Flight Dynamics Laboratory, under project 1467, "Structural Analysis Methods," Task 146704, "Structural Fatigue and Fracture Analysis Methods for Aerospace Vehicles."

The authors wish to express their appreciation to Cadets G.J. Butson and D. Tieszen of the United States Air Force Academy for their assistance during the testing and data acquisition phases of this effort.

The manuscript was released by the authors in February 1971.

This Technical Memorandum has been reviewed and is approved.

FRANCIS J. JANIK, JR.
Chief, Solid Mechanics Branch
Structures Division

TABLE OF CONTENTS

LIST OF FIGURES

TABLES

ABSTRACT

This report contains the results of spectrum crack growth tests of surface flawed D6ac plate materials. All spectra used in the program represented the critical wing pivot locations for the F-111 aircraft and were applied in a randomized block sequence containing 58 layers representing 200 flight hours. The effects of limited compression and the single overload proof test cycle were evaluated.

I. Introduction

As part of the overall effort to provide estimates of the safe crack growth period (inspection interval) following the static proof test of the F-111, the Air Force Flight Dynamics Laboratory has tested a limited number of surface flawed D6ac plate specimens under randomized block loading representing the Mission Analysis Composite (MAC) Spectrum for the aircraft wing pivot fitting (WPF) critical location. The primary objective of the test program was to establish the effect of the proof stress cycle on subsequent crack growth. In addition to this, limited variation in spectrum severity including compression was investigated.

Three basic versions of the MAC spectrum were used:

5g - Tension-Tension

7.33g - Tension-Tension

7.33g - Tension-Compression

This report describes the test program and presents the results. Analytical correlation efforts are currently being conducted and will be reported at a later date.

II Experimental Program

1. Specimen Description

Figure 1 includes the dimensions of the test specimen used throughout this program. The rectangular "starter flaw" was produced by the Elox (EDM) process to the dimensions indicated. Test machine capacity (50,000 lbs) limited the cross sectional area of the specimen to 0.3 in^2. The 0.3 in. thickness is representative of the critical Wing Pivot Fitting (WPF) location.

In order to minimize specimen size effects (i.e. width, and net section) material of medium toughness was specified (K_{IC} = 50 - 70KSi $\sqrt{in.}$) Unfortunately, several of the specimens were suspected of having K_{IC} values in the 80-90 KSi $\sqrt{in.}$ range, thus allowing total crack growth to approach the back surface. At the completion of testing, compact tension specimens were fabricated from the broken halves for the purpose of determining K_{IC} values.

2. Test Equipment and Environment

All testing was conducted on an MTS model 311.31 located in Building 65 at Wright-Patterson AFB, Ohio. This basic load frame has a capacity of 200 KIPS static and 100 KIPS dynamic loading; however, 50 KIP hydraulic grips were used throughout this program. All tests were conducted in laboratory air between June and October 1970. Relative humidity ranging between 40-90 percent can be expected during this time period. All spectrum tests were run at a rate of 5 Hertz. Precracking was conducted at a rate no greater than 9 Hertz.

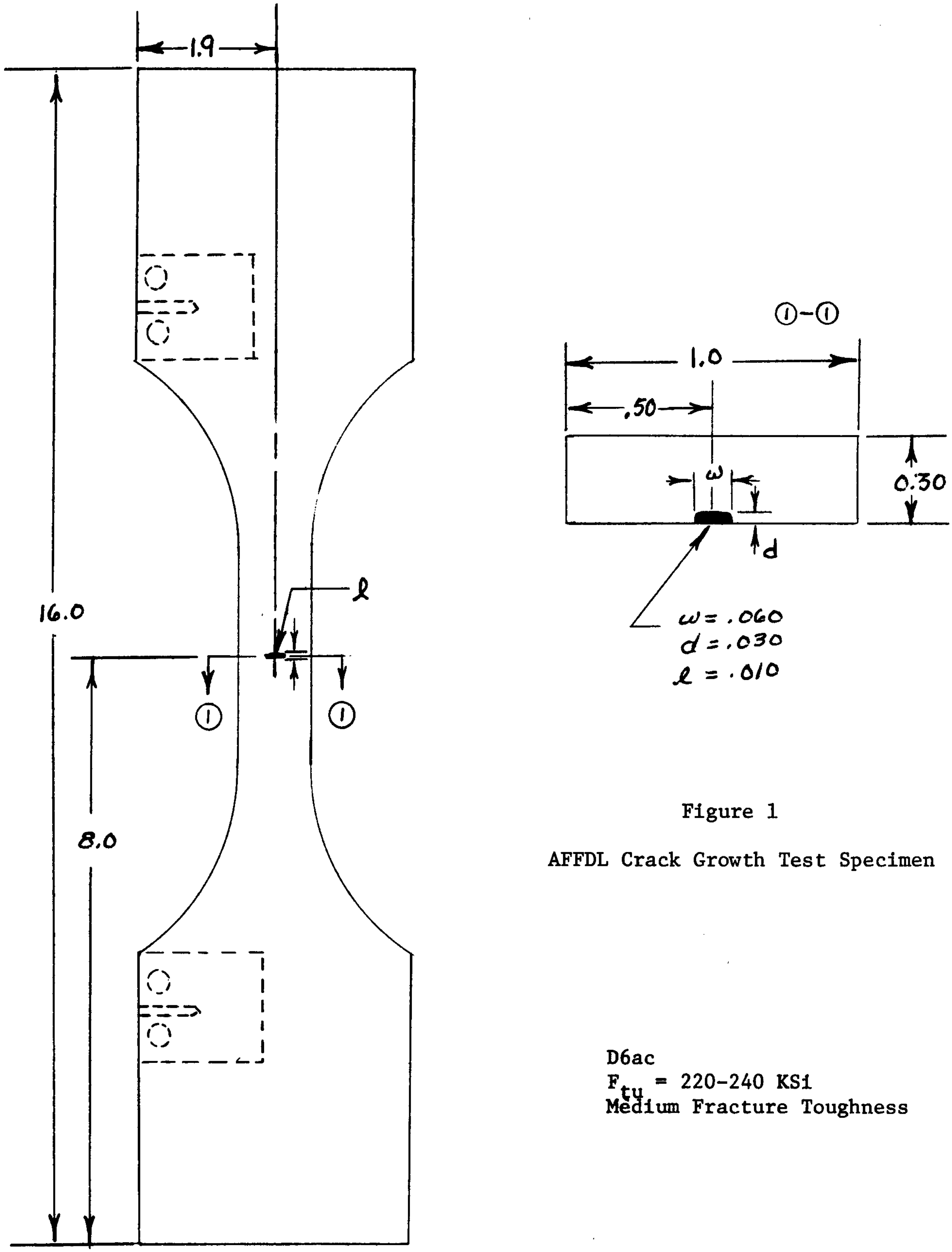

Figure 1

AFFDL Crack Growth Test Specimen

D6ac
F_{tu} = 220-240 KSi
Medium Fracture Toughness

3. Instrumentation

No special instrumentation was used to measure crack growth during the tests. For the initial specimens, growth was monitored by a 30X binocular microscope utilizing a strobe light and calibrated eye piece. This procedure was dropped, however, except to observe the precracking, since more accurate measurements of growth were available after the test from the striations on the fracture surface.

4. Loading

The randomized block loading MAC wing pivot fitting stress spectra were obtained from General Dynamics, Fort Worth, and are contained in Table Ia, b, c. Each tabulation or block is representative of 200 flight hours. The 7.33g Tension-Compression spectrum was derived by modifying the basic 7.33g spectrum (Table Ib) to include the representative number of occurrences of negative load factor obtained from Reference 1. This loading sequence was programmed as input on paper tape into a digital computing simulator, (Information Technology, Inc.) model no. ITI 4901. The ITI simulates the spectrum loading as required and was used chiefly as a storage bank from which the loads could be repeatedly recalled in the form of 3 outputs of varying D.C. signals. The first channel was the actual load input which initially went through a limiting control circuit, set at 1% over the maximum load cycle. From this circuit, the signal was input as a demand function into a servo controller amplifier which controlled the test load. The output of channel number 2 was a verification of the mean load changes in the block spectrum, and also allowed verification of the number of cycles in each layer. The

TABLE Ia CONDENSED MAC SPECTRUM WPF

Layer No.	σ_{min}	σ_{max}	n	Layer No.	σ_{min}	σ_{max}	n
1	0.2	48.0	63	34	22.8	106.6	1
2	20.3	77.9	76	35	4.7	18.3	265
3	1.3	39.5	371	36	2.3	59.9	34
4	17.0	76.0	37	37	22.5	58.1	318
5	2.3	50.5	111	38	10.6	34.2	6
6	30.6	73.2	2	39	0	32.7	21
7	2.2	40.8	363	40	20.7	51.7	374
8	11.6	82.6	5	41	5.8	40.0	478
9	10.5	30.7	1280	42	4.6	25.4	46
10	19.5	65.9	62	43	0.2	34.2	300
11	10.5	47.9	1	44	4.6	32.6	10
12	17.5	50.5	89	45	22.8	91.4	4
13	24.9	63.0	41	46	0	47.2	4
14	27.4	55.2	57	47	21.8	41.9	306
15	10.9	40.4	491	48	23.8	71.8	15
16	0	40.2	6	49	23.0	75.2	5
17	11.0	50.4	74	50	23.6	37.3	230
18	22.7	38.7	682	51	23.0	31.0	1338
19	2.1	29.9	1376	52	0.2	57.2	19
20	27.0	46.1	66	53	11.1	29.9	1546
21	1.5	49.7	34	54	0	18.4	238
22	19.5	24.8	1621	55	1.4	46.4	114
23	23.0	33.9	1589	56	20.4	43.1	370
24	1.3	30.7	1374	57	11.1	59.9	7
25	0	25.4	67	58	5.8	40.0	478
26	20.4	82.0	1				
27	21.3	65.7	250				
28	0.2	63.8	8				
29	4.7	40.1	2				
30	22.9	100.7	2				
31	10.5	46.3	37				
32	21.8	48.3	367				
33	20.6	73.9	109				

TABLE Ib CONDENSED MAC SPECTRUM WPF
7.33g Tension-Tension

Layer No	σmin	σmax	n	Layer No.	σmin	σmax	n
1	0.2	48.0	63	37	0.2	63.8	8
2	20.3	77.9	76	38	4.7	40.1	2
3	1.3	39.5	371	39	22.9	100.7	2
4	17.0	76.0	37	40	10.5	46.3	37
5	2.3	50.5	111	41	21.8	48.3	367
6	30.6	73.2	2	42	11.5	102.3	1
7	2.2	40.8	363	43	20.6	73.9	109
8	11.6	82.6	5	44	22.8	106.6	1
9	10.5	30.7	1280	45	4.7	18.3	265
10	23.2	80.4	1	46	2.3	59.9	34
11	19.5	65.9	62	47	22.5	58.1	318
12	10.5	47.9	1	48	10.6	34.2	6
13	17.5	50.5	89	49	0.0	32.7	21
14	20.4	90.2	1	50	20.7	51.7	374
15	24.9	63.0	41	51	5.8	40.0	478
16	27.4	55.2	57	52	4.6	25.4	46
17	10.9	40.4	491	53	0.2	34.2	300
18	10.2	51.6	7	54	4.6	32.6	10
19	0.0	40.2	6	55	22.8	91.4	4
20	11.0	50.4	74	56	0.0	47.2	4
21	22.7	38.7	682	57	21.8	41.9	306
22	20.1	67.5	4	58	23.8	71.8	15
23	2.1	29.9	1376	59	23.0	75.2	5
24	20.4	82.2	5	60	23.6	37.3	230
25	27.0	46.1	66	61	23.0	31.0	1338
26	1.5	49.7	34	62	0.2	57.2	19
27	19.5	24.8	1621	63	11.1	29.9	1546
28	20.4	82.2	5	64	0.0	18.4	238
29	23.0	33.9	1589	65	1.4	46.4	114
30	20.4	85.6	2	66	20.4	43.1	370
31	1.3	30.7	1374	67	11.1	59.9	7
32	22.9	108.3	1	68	5.8	40.0	478
33	0.0	25.4	67				
34	20.4	82.0	1				
35	21.3	65.7	250				
36	11.5	93.7	2				

TABLE Ic CONDENSED MAC SPECTRUM WPF
7.33g Tension-Compression*

Layer No.	σ_{min}	σ_{max}	n	Layer No.	σ_{min}	σ_{max}	n
1	0.2	48.0	63	36	-20.0	93.7	1
2	20.3	77.9	76	37	0.2	63.8	8
3	1.3	39.5	371	38	11.5	93.7	1
4	17.0	76.0	37	39	4.7	40.1	2
5	2.3	50.5	111	40	22.9	100.7	2
6	30.6	73.2	2	41	10.5	46.3	37
7	2.2	40.8	363	42	21.8	48.3	367
8	11.6	82.6	5	43	-24.0	102.3	1
9	10.5	30.7	1280	44	20.6	73.9	109
10	23.2	80.4	1	45	22.8	106.6	1
11	19.5	65.9	62	46	4.7	18.3	265
12	10.5	47.9	1	47	2.3	59.9	34
13	17.5	50.5	89	48	22.5	58.1	318
14	20.4	90.2	1	49	10.6	34.2	6
15	24.9	63.0	41	50	-4.0	32.7	21
16	27.4	55.2	57	51	20.7	51.7	374
17	10.9	40.4	491	52	5.8	40.0	478
18	10.2	51.6	7	53	4.6	25.4	46
19	0.0	40.2	6	54	0.2	34.2	300
20	11.0	50.4	74	55	4.6	32.6	10
21	22.7	38.7	682	56	22.8	91.4	4
22	-12.0	67.5	4	57	0.0	47.2	4
23	2.1	29.9	1376	58	21.8	41.9	306
24	20.4	82.2	5	59	23.8	71.8	15
25	27.0	46.1	66	60	23.0	75.2	5
26	1.5	49.7	34	61	23.6	37.3	230
27	19.5	24.8	1621	62	23.0	31.0	1338
28	20.4	82.2	5	63	0.2	57.2	19
29	23.0	33.9	1589	64	11.1	29.9	1546
30	20.4	85.6	2	65	0.0	18.4	238
31	1.3	30.7	1374	66	1.4	46.4	114
32	22.9	108.3	1	67	20.4	43.1	370
33	0.0	25.4	67	68	11.1	49.9	7
34	20.4	82.0	1	69	5.8	40.0	478
35	21.3	65.7	250				

* Occurrences of negative loads derived from Table III of Reference I

third channel was used to trigger the strobe light synchronous with the maximum peak of each individual stress amplitude cycle. Continuous monitoring of the loading was accomplished with a two channel Sanborn recorder.

5. Testing Procedure

Upon insertion of the test specimens into the loading grips, the elox slot was cleansed of all foreign matter using compressed air. This insured maximum visual observation of the slot depth during the precracking operation. The surface of the specimen was not altered in any manner.

Precracking was accomplished using a constant amplitude stress range of 1.6 - 70 Ksi and a rate not greater than 9 Hertz. Crack initiation was observed using a binocular microscope as previously mentioned. For those specimens which were not to receive a proof test, precracking was concluded at the first indication of cracking in the slot. For the proof tested samples, precrack growth was allowed to progress to a preassigned surface length. A semicircular crack was assumed to have developed. Proof loads were applied manually with a complete cycle duration of approximately sixty seconds. Following the precracking or successful proof test, the system was switched to the ITI for automatic spectrum cycling to failure.

One specimen was cycled in a dry nitrogen environment to establish a basis for comparison. This was accomplished by purging a fabricated plexiglas enclosure with dry nitrogen gas throughout

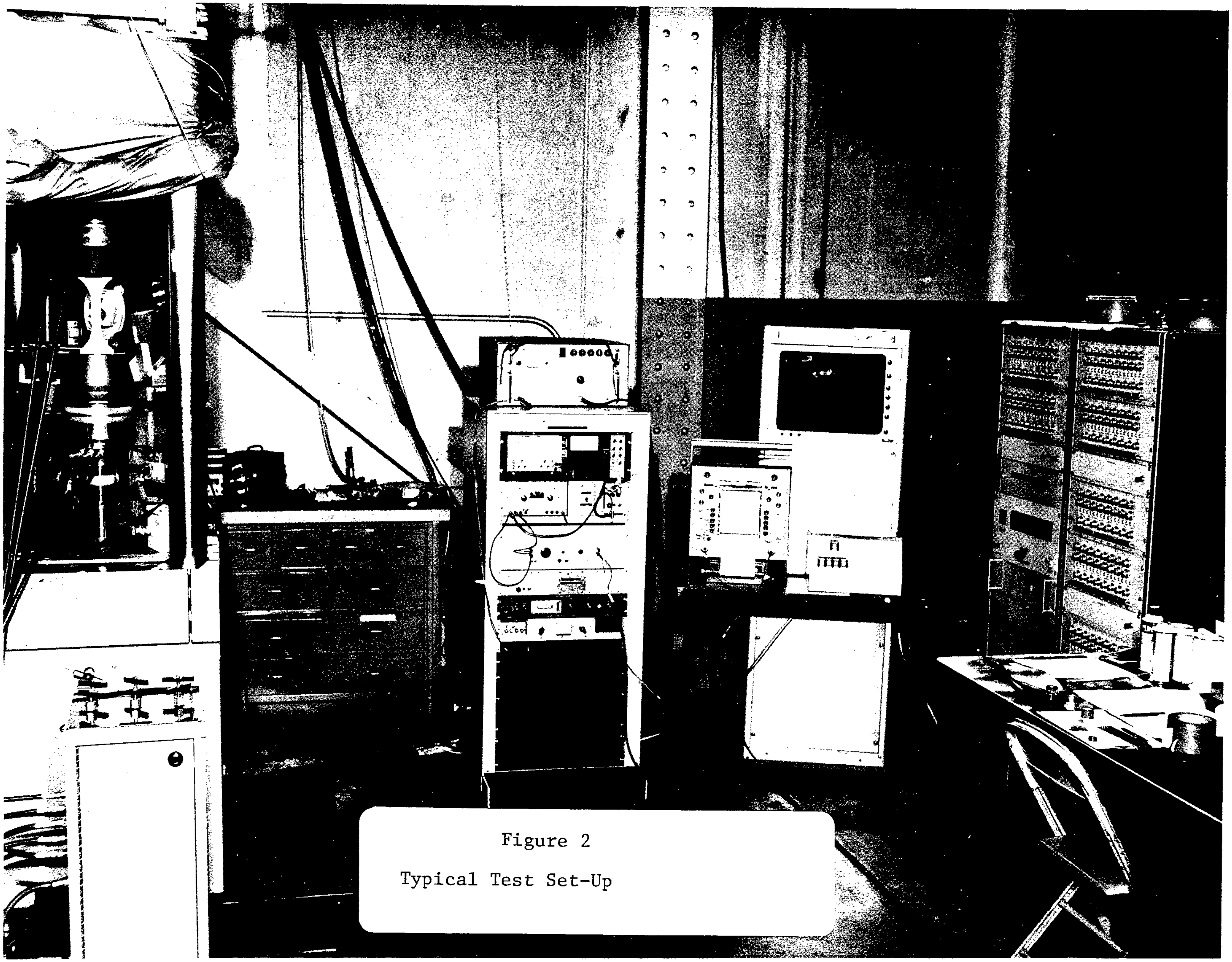

Figure 2

Typical Test Set-Up

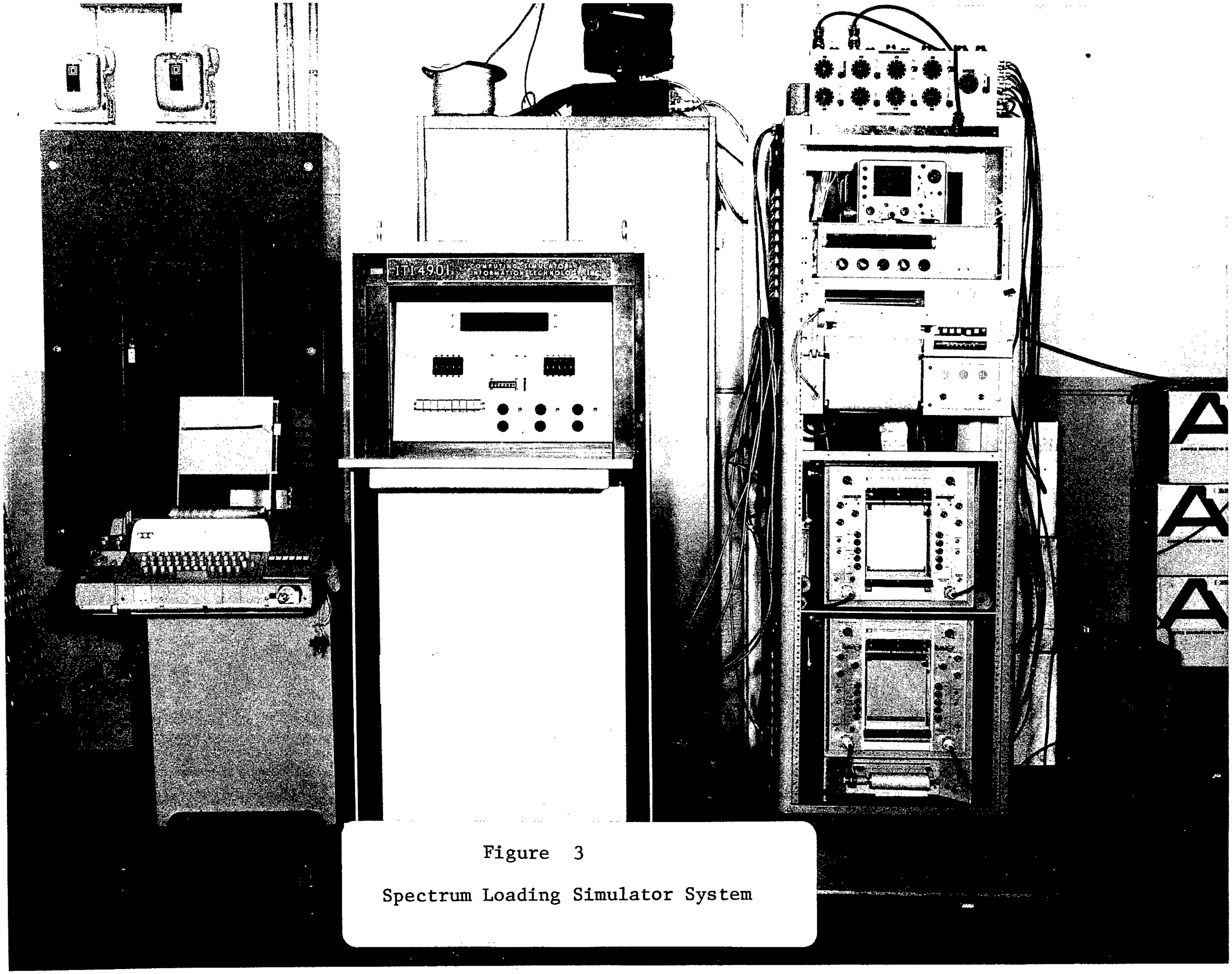

Figure 3

Spectrum Loading Simulator System

the test. A similar fixture was employed for the cold proof tests, however, the gas was cycled through a pool of liquid nitrogen. During the cool down, temperatures were monitored with thermocouples mounted on both the front and back surfaces of the specimen. All cold proof tests were conducted at a nominal -40°F. The specimen was allowed to return to room temperature before cycling.

All testing was performed in two consecutive eight hour shifts. At the end of each day, the specimen was removed and stored in a dry atmosphere container. After failure, the fracture surfaces were protected with machine oil or Krylon silicon spray.

The precrack limits for the proof tested specimens were determined by assuming growth of a semicircular flaw and calculating the depth "a" and surface length "2c" from the expression:

$$a = \left(\frac{K_{IC}}{1.1\sigma_p}\right)^2 Q/\pi = c$$

A toughness value of K_{IC} = 55 Ksi $\sqrt{in.}$ was assumed for the room temperature condition and K_{IC} = 50 Ksi $\sqrt{in.}$ for the cold (-40°F) proof tests. With the limit proof stress level of σ_p = 146Ksi (representative of the wing pivot fitting location), crack depths of the following dimensions were determined:

Room temperature	a =.071 in., 2c = .142 in
-40°F	a = .059 in., 2c = .118 in.

6. <u>Data Interpretation</u>

All pertinent fracture surface data was charted using a Gaertner tool makers measuring microscope (-100X). Readings of 0.0001 in. are possible with this instrument.

Convenient marker bands were produced on the fracture surface by the higher stress applications of the spectrum and were used to identify individual blocks. Other details such as the end of precracking and application of the single proof test cycle were generally recognized with this technique. In addition to the optical microscope, a scanning Electron Microscope was used. This device allowed more accurate interpretation of the "early" blocks (not normally distinguishable by optical means.) Figure 4a and 4b includes typical results from the Scanning Electron Microscope where layers 30 or 34 of the 5g spectrum are readily identified. Figure 4c includes a 100X composite of one half the cracked surface for a typical specimen obtained with the Scanning Electron Microscope.

100X

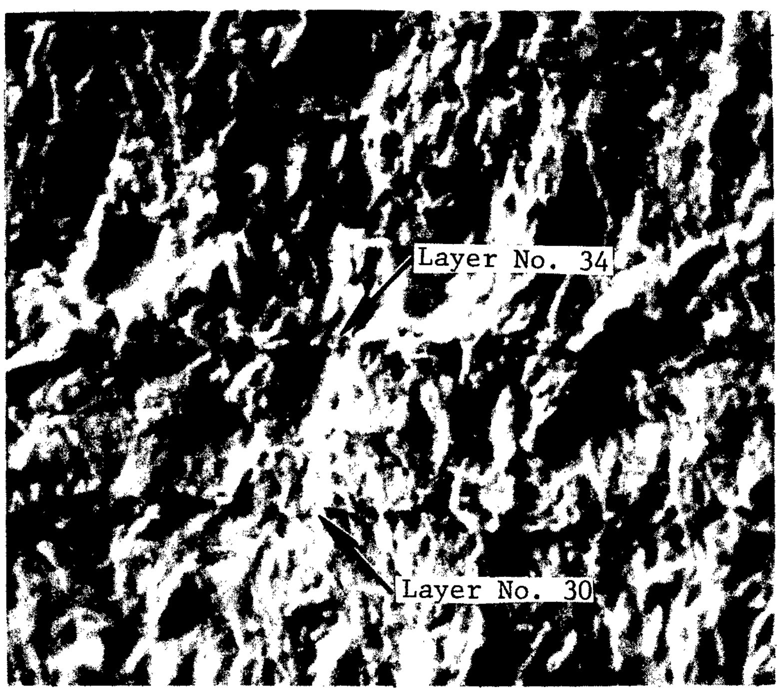

1000X

Figure 4 Scanning Electron Microscope Photographs

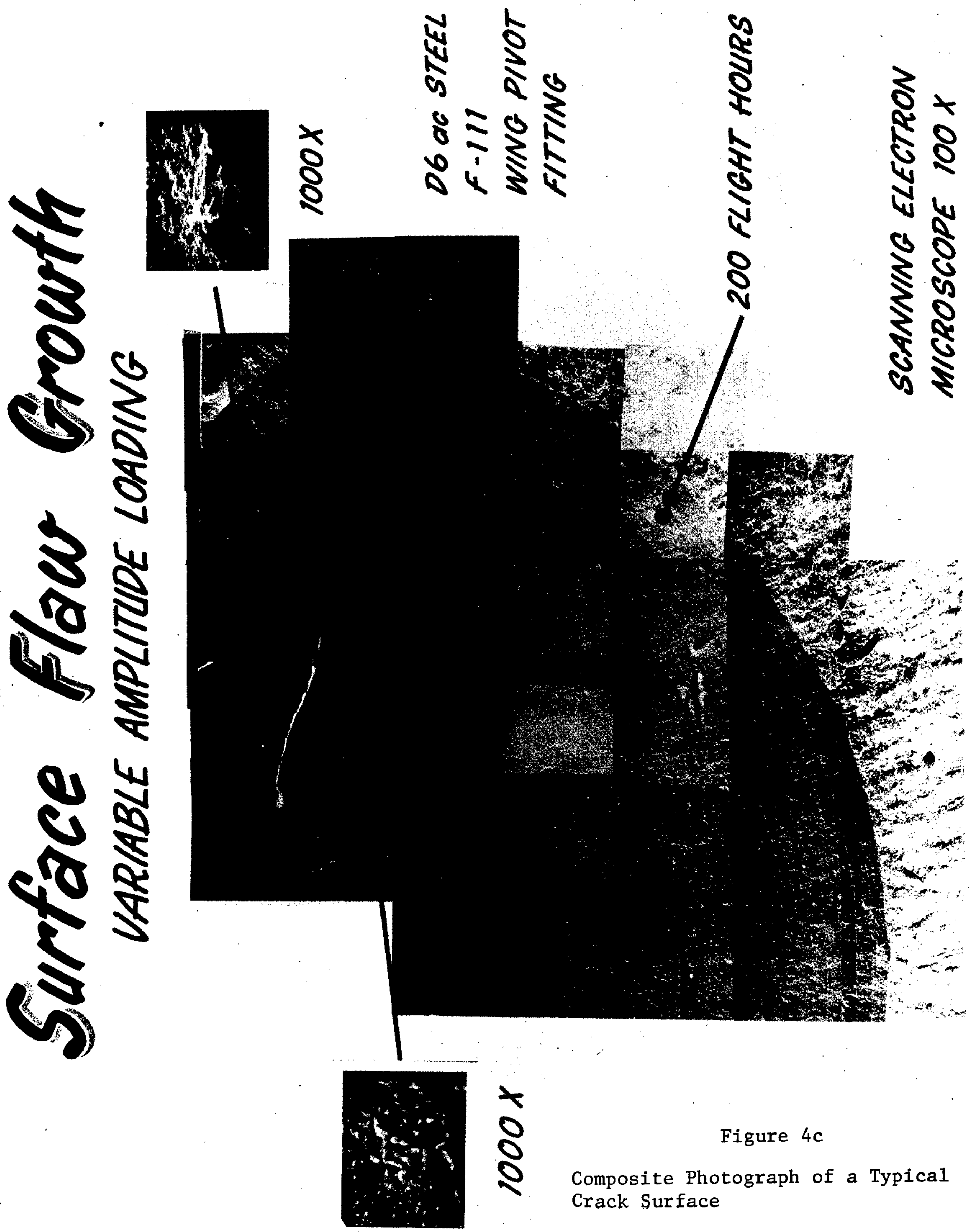

Figure 4c

Composite Photograph of a Typical Crack Surface

III Experimental Results

Table IV contains the measured crack depth "a" for individual blocks of testing. In all cases, this measurement was made from the specimen surface to the band produced by layer 30 of the spectra. Plots of this data are contained in Figures 5 through 20. Final fracture dimensions for each specimen are summarized in Table III. Table II contains a detailed summary of important test results and includes estimates of the stress intensity factor K_Q at the point of fracture.

Table V contains the compact tension results for K_{IC} for the majority of the test specimens. These specimens were removed from the broken halves as indicated in Figure 1. All K_{IC} testing was conducted by the Air Force Materials Laboratory (LAE).

Table II - Test Summary

Specimen No.	Initial Crack Depth	Final Crack Depth	Total Blocks to Failure	Spectrum	Fracture Stress	Final Crack Width	$a_f/2c_f$	$c_f/2a_f$	K_Q*	K_P**	Remarks
	a_o	a_f	N_f		σ_{GF}	$2C_f$					
P3F2	0.116	.198	13	5g	142	.374	.53	.47	81		R.T.-Laboratory Air
P3F3	0.122	.227	18	5g	100.7	.434	.52	.48	61		"
P1M14	0.14	.195	12	5g	106	.345	.57	.43	62		"
P1M15	0.062	.203	78	5g	100.7	.318	.64	.36	64		"
P1M16	0.083	.200	62	5g	112	.324	.62	.38	69		R.T.-Dry Nitrogen
P3G2	0.096	.268	42	5g	106	.603	.44	.56	72	58	R.T. Proof Test (1)
P1M13	0.161	.238	19	5g	100.7	.403	.59	.41	66	75	R.T. Proof Test (1)
P1D12	0.158	.158	0	5g	105 (2)	.258	.61	.49	53	53	-40° Proof Test (failed in test)(2)
P1D11	0.061	.206	69 (3)	5g	100.7	.366	.56	.44	59	45	-40° Proof Test (2 proof tests) (1)
P1D13	.090	.183	36	5g	100.7	.317	.58	.42	58	55	-40° Proof Test (1)
P5I10	.048	.228	112	7.33g T-T	106.6	.437	.52	.48	65		R.T.-Lab. Air 7.33g T-T MAC

Table II - Test Summary (cont'd)

Specimen No.	Initial Crack Depth	Final Crack Depth	Total Blocks to Failure	Spectrum	Fracture Stress	Final Crack Width	$a_f/2c_f$	$c_f/2a_f$	K_Q*	K_P**	Remarks
	a_o	a_f	N_f		σ_{GF}	$2C_f$					
P5I9	.088	.275	73	7.33 T-C	108.3	.583	.47	.53	73		R.T. - Lab Air 7.33g T-C MAC
P3G3	.052	.200	82	7.33 T-C	108.3	.351	.57	.43	61		R.T.-Lab Air 7.33g T-C MAC

Notes: (1) Proof test stress = 146 KSi
(2) Proof test stress = 105 KSi
(3) After 2nd proof test

* $K_Q = 1.1\ \sigma_{GF} \sqrt{\pi(a_f/Q)}$

** K_P = Estimated K during proof stress

Table III Fracture Surface Geometry

	P3F2	F3G2	PcF3	P1D11	P1M15	P1D12	P1M14	P1M13	P1M16	P1D13
$2C_f$	.374	.603	.434	.366	.318	.258	.345	.403	.324	.317
$2C_S$	.312	.532	.394	.226	.291	.188	.297	.321	.267	.259
a_f	.198	.268	.227	.206	.203	.158	.195	.238	.200	.183
W	.060	.061	.060	.097	.060	.064	.061	.061	.061	.059
d	.030	.030	.027	.030	.033	.008	.032	.030	.033	.032
S_1	.118	.184	.077	.059	.00	.059	.098	.118	.041	.072
S_2	.104	.222	.076	.101	.00	.053	.099	.117	.052	.084
ℓ_1	.052	.080	.023	.014	.015	.011	.022	.019	.020	.015
ℓ_2	.049	.049	.027	.014	.007	.009	.018	.019	.018	.017
ℓ_3	.412	.395	.366	.397	.320	.432	.421	.409	.394	.421
ℓ_4	.423	.397	.344	.421	.325	.421	.423	.413	.414	.418
ℓ_5	.045	.033	.026	.021	.023	.014	.025	.024	.027	.019
ℓ_6	.032	.031	.013	.010	.017	.011	.007	.007	.018	.008
ℓ_7	.049	.031	.030	.019	.024	.011	.023	.024	.035	.021
t	.300	.300	.301	.301	.294	.297	.305	.297	.297	.295
w	.987	.992	.990	.999	.990	.996	.990	.990	.991	.997

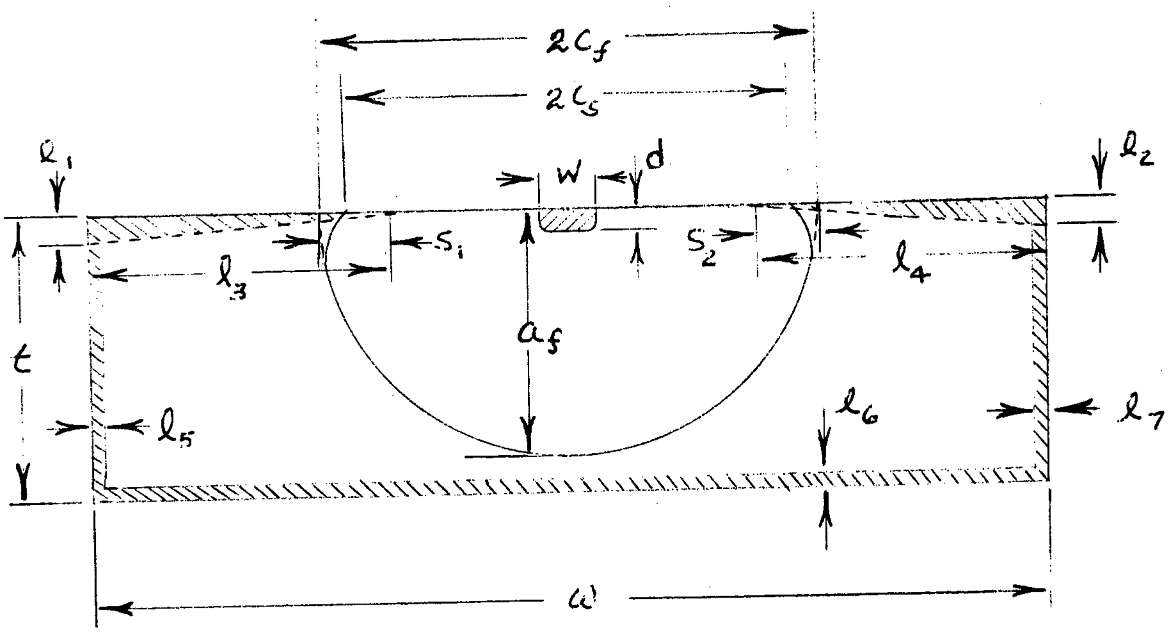

Table III Fracture Surface Geometry (cont'd)

	P5I10	P5I9	P3G3
2Cf	.437	.583	.351
$2C_S$	.396	.543	.298
af	.228	.275	.200
W	.062	.060	.063
d	.033	.031	.032
S_1	.157	.247	.123
S_2	.247	.248	.138
ℓ_1	.024	.049	.024
ℓ_2	.023	.055	.020
ℓ_3	.444	.467	.451
ℓ_4	.520	.444	.456
ℓ_5	.034	.037	.031
ℓ_6	.013	.024	.015
ℓ_7	.025	.033	.034
t	.298	.297	.289
ω	.997	.999	.997

IV Data Analysis

1. Spectrum Growth

To indicate the variability of spectrum growth data, all non-proof tested 5g MAC spectrum data has been plotted in Figure 14. The data has been normalized to a common crack depth. The dry air data of specimen P1M16 has been included also to show the accelerating effects of humid laboratory air.

The effects of spectrum severity and limited compression may be seen in Figure 20 where the results of P1M15 have been compared with P5I10 (7.33g T-T) and P5I9 (7.33g T-C). For the particular ordering of the test spectrum used in this program, the occurrences of high stress in the 7.33g spectrum appear to have a retarding effect. Limited compression caused a more rapid growth; however, the results of P5I9 fall within the scatter of the 5g spectrum.

2. The Effect of Proof Stress

With the exception of specimen P1M13, no marked delay in crack growth was evident due to the prior application of the limit stress proof test. Comparative plots of the data have been included in Figures 15-18. Using fracture surface measurements, the approximate level of K_p, the estimated stress intensity for the proof stress application was determined. These results have been included in Table II. The results for P1M13 indicate the level of K_p higher than any other proof tested specimen. In fact, the reported results in Table II reveal a level greater than either K_Q or K_{IC}. This phenomenom may be attributed to stable growth during the proof test

cycle and that the observed crack length used to calculate K_p was actually that which resulted after the single overload cycle, including the stable portion. Stable growth during simulated proof testing has been observed in Titanium. (Reference 2)

3. Specimen Size Effects

As mentioned previously, specimen width in the program was restricted because of test machine capacity limitations. This requirement necessitated the generation of surface cracks of fairly sizeable area relative to nominal specimen cross sectional area. The resultant effect is to elevate the level of stress and produce, at fracture, an apparent K_Q less than K_{IC}. For growth testing, this effect should be minimal; however, since growth rate is primarily a function of range of stress or range of stress intensity, ΔK. Good agreement between these reported tests and others conducted on wider specimens using the same spectrum has been noted.

Nevertheless, some account should be made of the possible size effects when interpreting the reported data. The authors suggest the crack depth, a = 0.20, as the upper bound for reliable growth data. This cutoff does not in any way limit the effectiveness of the data.

4. Final Fracture

As indicated in Figure 4c and Table III, crack growth on the surface of the specimen was constrained apparently due to the presence of compressive residual stresses caused by the shot peening operation.

The apparent K_Q values listed in Table II are listed as a

matter of interest only, and have not been corrected to include specimen width or back surface effects.

Table IV - Surface Growth Measurements

P1D13				P1M13	
Block	a	Block	a	Block	a
a_0	.090	27	.142	Proof Test	.161
6	.097	28	.145	10	.171
7	.097	29	.150	11*	.174
8	.098	30	.155	12	.178
9	.099	31	.159	13	.184
10	.101	32	.164	14	.190
11	.102	33	.168	15	.197
12	.104	34	.173	16	.205
13	.106	35	.179	17	.214
14	.108	36	.183	18	.225
15	.110			19	.238
16	.112				
17	.114				
18	.116				
19	.118				
20	.121				
21	.124				
22	.126				
23	.130				
24	.132				
25	.135				
26	.139				

*Note: A spike followed by a compressive load occurred in Block 11

Table IV - Surface Growth Measurements

P1D11			
Block	a	Block	a
a_c AFTER 2nd Proof Test	.061	52	.124
32	.084	53	.127
33	.086	54	.130
34	.087	55	.133
35	.088	56	.136
36	.090	57	.140
37	.092	58	.144
38	.093	59	.148
39	.095	60	.152
40	.096	61	.156
41	.098	62	.162
42	.100	63	.166
43	.102	64	.172
44	.104	65	.178
45	.106	66	.184
46	.108	67	.191
47	.111	68	.198
48	.113	69	.206
49	.116		
50	.119		
51	.122		

Table IV - Surface Growth Measurements

P1M16			
Block	a	Block	a
a_o	.083		
27	.107	49	.145
28	.108	50	.148
29	.108	51	.150
30	.109	52	.153
31	.110	53	.156
32	.112	54	.159
33	.113	55	.163
34	.114	56	.166
35	.116	57	.169
36	.118	58	.173
37	.119	59	.177
38	.121	60	.181
39	.123	61	.186
40	.125	62	.190
41	.127	a_f	.200
42	.129		
43	.131		
44	.133		
45	.135		
46	.137		
47	.140		
48	.143		

Table IV - Surface Growth Measurements

P1M15			
Block	a	Block	a
a_o	.062	65	.142
44	.100	66	.146
45	.101	67	.149
46	.102	68	.152
47	.104	69	.156
48	.105	70	.159
49	.107	71	.164
50	.109	72	.168
51	.111	73	.173
52	.112	74	.178
53	.114	75	.183
54	.116	76	.189
55	.118	77	.195
56	.120	78	.203
57	.122		
58	.124		
59	.127		
60	.129		
61	.131		
62	.134		
63	.137		
64	.139		

Table IV - Surface Growth Measurements

P3G2			
Block	a	Block	a
a_o	.096	31	.175
11	----	32	.181
12	----	33	.188
13	----	34	.195
14	----	35	.203
15	----	36	.211
16	.115	37	.220
17	.117	38	.229
18	.121	39	.241
19	.124	40	.252
20	.127	41	.265
21	.130	a_f	.268
22	.134		
23	.137		
24	.142		
25	.146		
26	.150		
27	.154		
28	.159		
29	.165		
30	.170		

Table IV - Surface Growth Measurements

P1M14		P3F2		P3F3	
Block	a	Block	a	Block	a
1	.143	a_o	---	a_o	.123
2	.147	1	---	1	.127
3	.151	2	.124	2*	.131
4	.155	3	.129	3*	.135
5	.159	4	.133	4*	.139
6	.163	5	.137	5	.142
7	.168	6	.142	6	.146
8	.173	7	.146	7	.151
9	.179	8	.151	8	.156
10	.185	9	.156	9*	.162
11*	.194	10	.162	10	.168
a_f	.195	11	.169	11	.174
		12	.175	12	.180
		13	.184	13	.186
			.187	14	.193
			.193	15	.200
				16	.208
				17	.217
				18	.228
*Compressive load occurred in Block 11 The computer was re-programmed and Block 11 was started over.		Note: Overload occured near end of Block 13 and specimen was pulled to failure at a high stress level		*Extra 100 cycles in Layer 4 of Mac Spec-trum in these Blocks	

Table IV - Surface Growth Measurements

P5I9			
Block	a	Block	a
41	.115	62	.186
42	.117	63	.191
43	.119	64	.198
44	.122	65	.204
45	.124	66	.211
46	.127	67	.218
47	.130	68	.226
48	.132	69	.234
49	.135	70	.244
50	.138	71	.254
51	.141	72	.266
52	.144	a_f	.275
53	.147		
54	.151		
55	.155		
56	.158		
57	.162		
58	.167		
59	.171		
60	.176		
61	.180		

Table IV - Surface Growth Measurements

P5I10				P3G3	
Block	a	Block	a	Block	a
79	.115	99	.165	63	.128
80	.117	100	.168	64	.130
81	.119	101	.172	65	.132
82	.121	102	.176	66	.134
83	.123	103	.180	67	.136
84	.125	104	.184	68	.139
85	.127	105	.188	69	.142
86	.129	106	.193	70	.145
87	.131	107	.198	71	.148
88	.134	108	.203	72	.152
89	.136	109	.208	73	.156
90	.139	110	.214	74	.160
91	.141	111	.220	75	.164
92	.144	a_f	.228	76	.168
93	.146			77	.173
94	.149			78	.178
95	.152			79	.183
96	.155			80	.188
97	.158			81	.194
98	.161			a_f	.200

TABLE V Compact Tension Test Results (K_{IC})

Specimen	Location(1)	K_{IC}	K_Q(2)
P1M13	-1	61.0	66
	-2	59.0	
P1M16	-1	59.8	
	-2	52.4	69
P3G2	-1	----	
	-2	76.0	72
P3F2	-1	69.6	
	-2	----	81
P3F3	-1	68.3	
	-2	76.4	61
P1M14	-1	47.8	
	-2	62.0	62
P1D11		61.9	59
P1D12		63.4	53
P1D13		61.1	58

(1) -1,-2 indicate 1 specimen from each broken half

(2) Surface flaw fracture level - See Table II

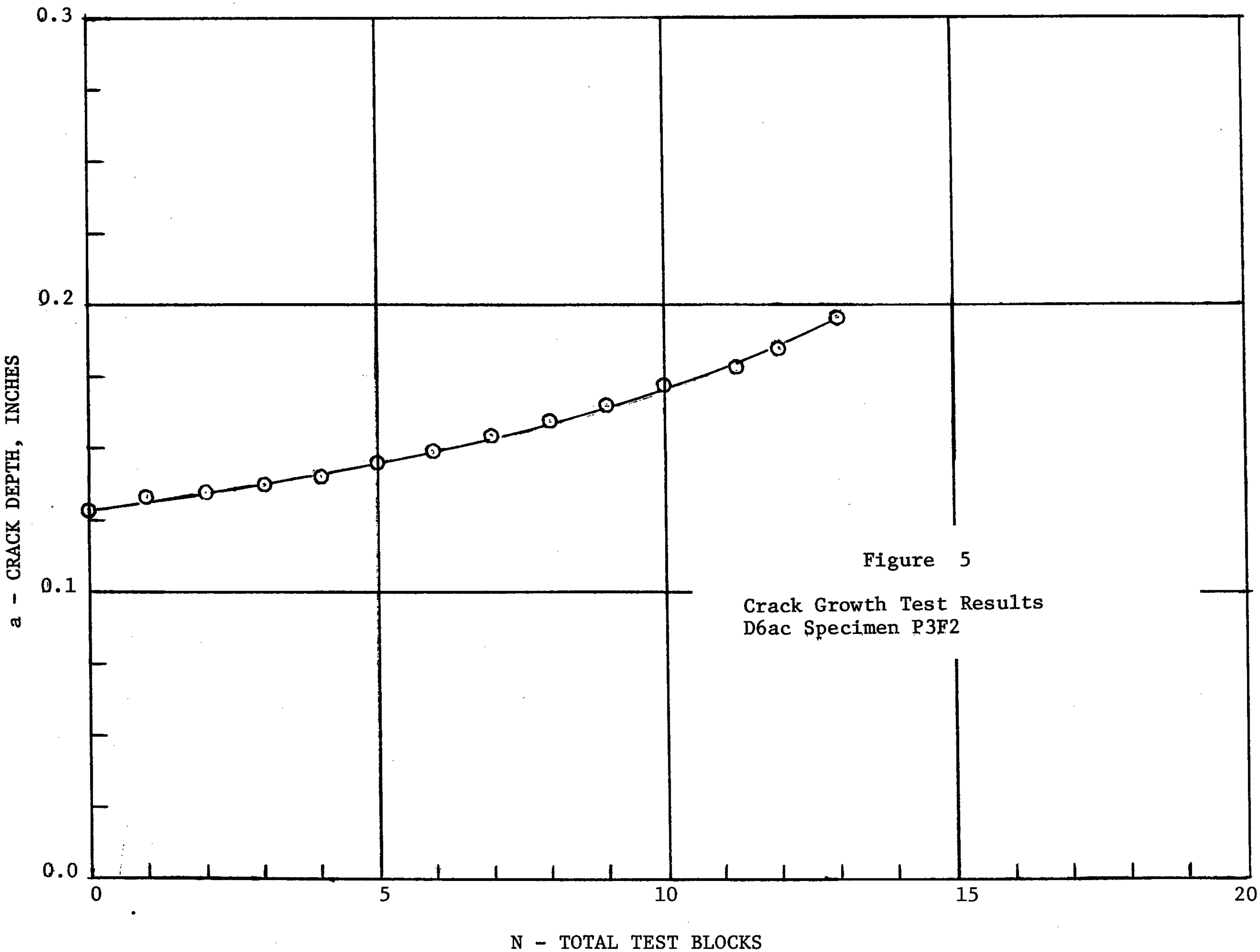

Figure 5

Crack Growth Test Results
D6ac Specimen P3F2

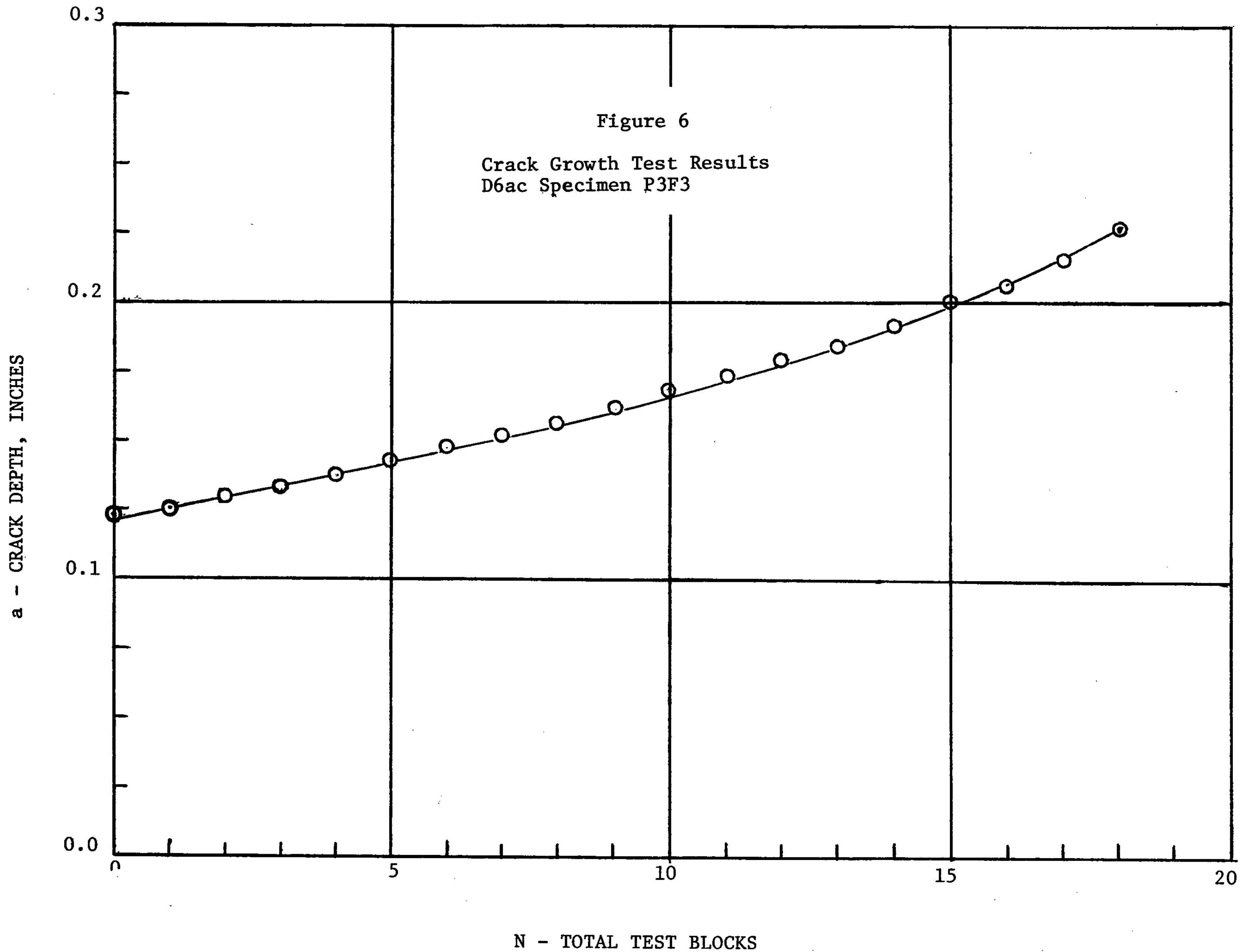

Figure 6

Crack Growth Test Results
D6ac Specimen P3F3

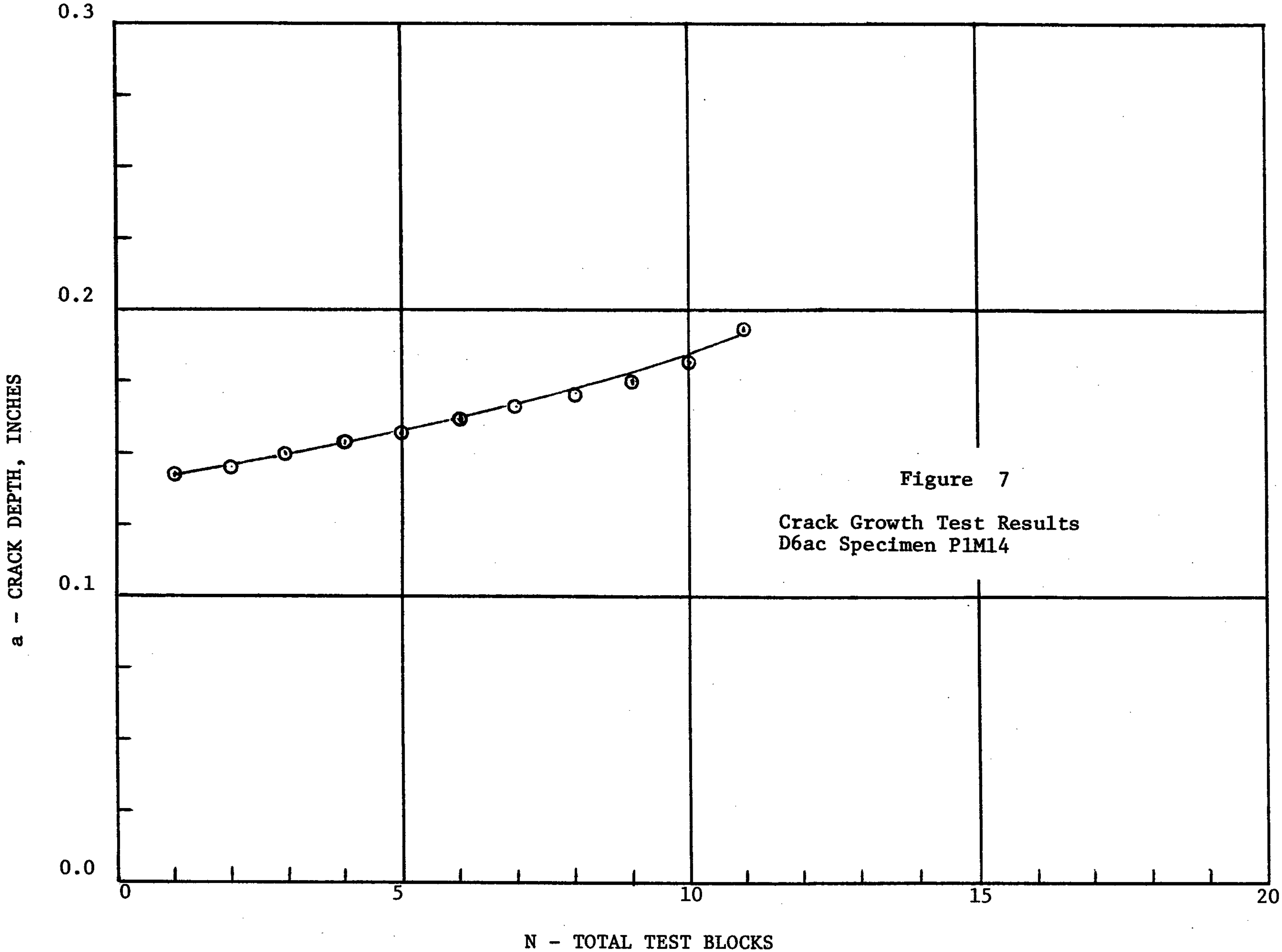

Figure 7

Crack Growth Test Results
D6ac Specimen P1M14

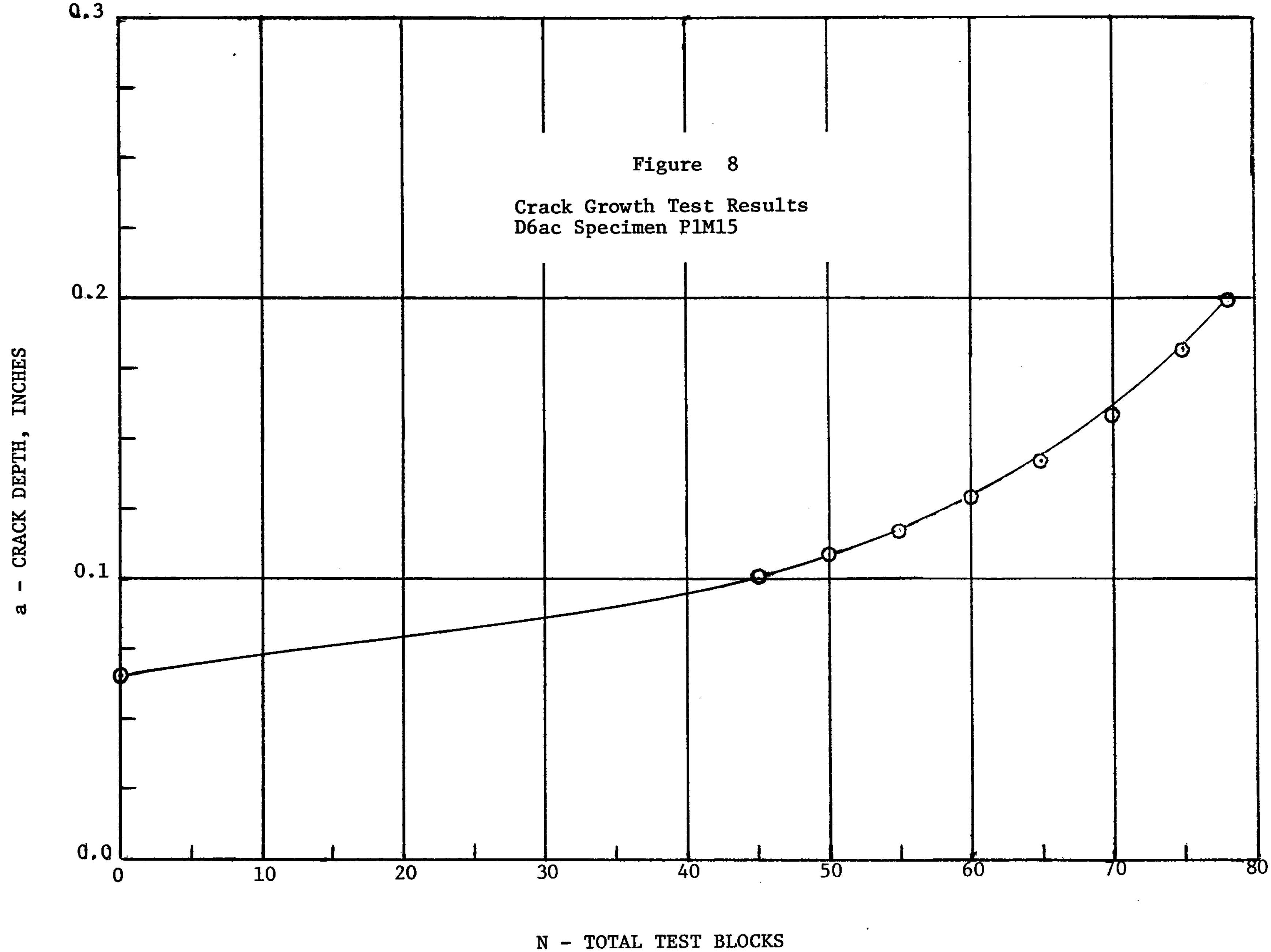

Figure 8

Crack Growth Test Results
D6ac Specimen P1M15

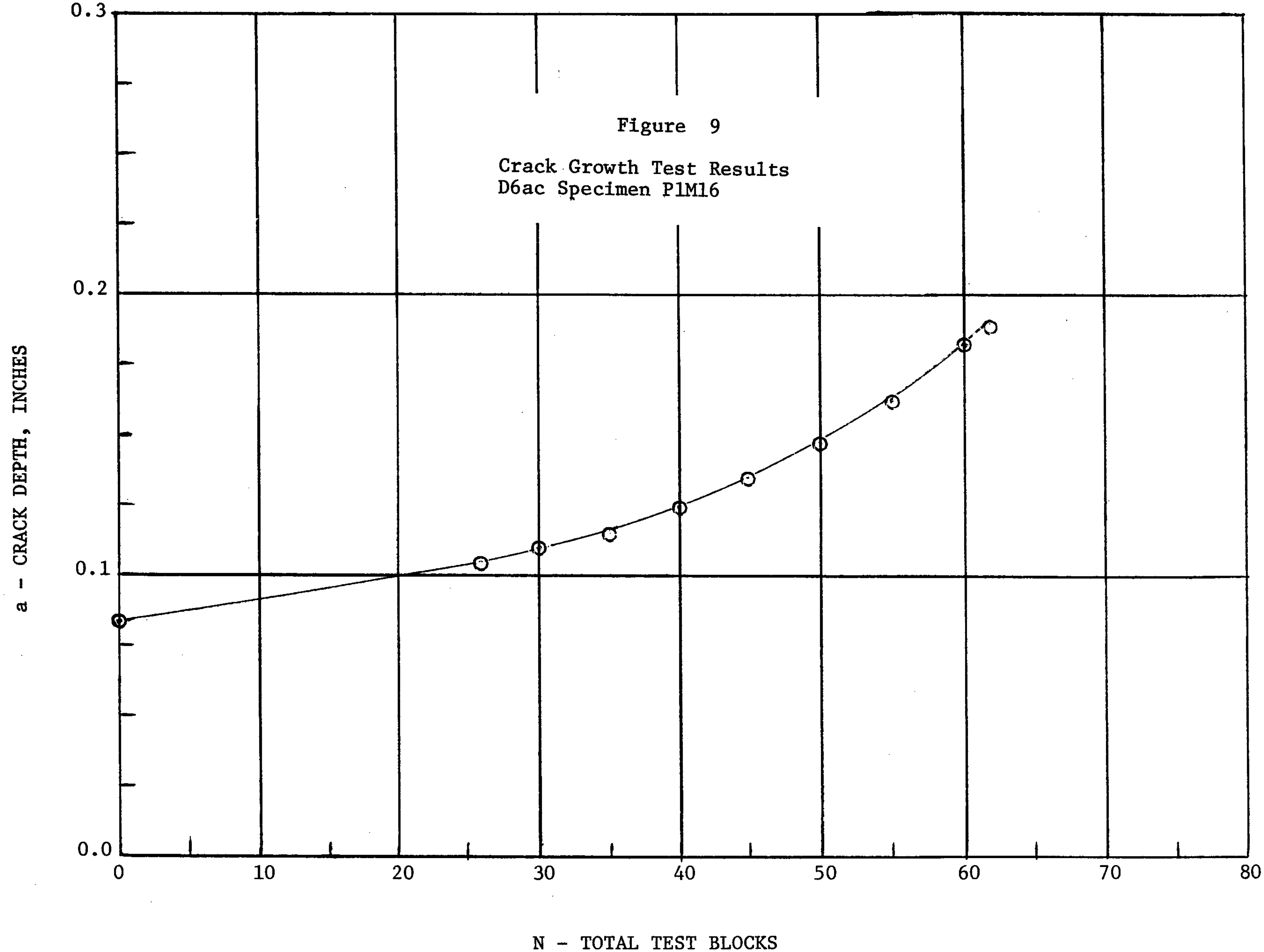

Figure 9

Crack Growth Test Results
D6ac Specimen P1M16

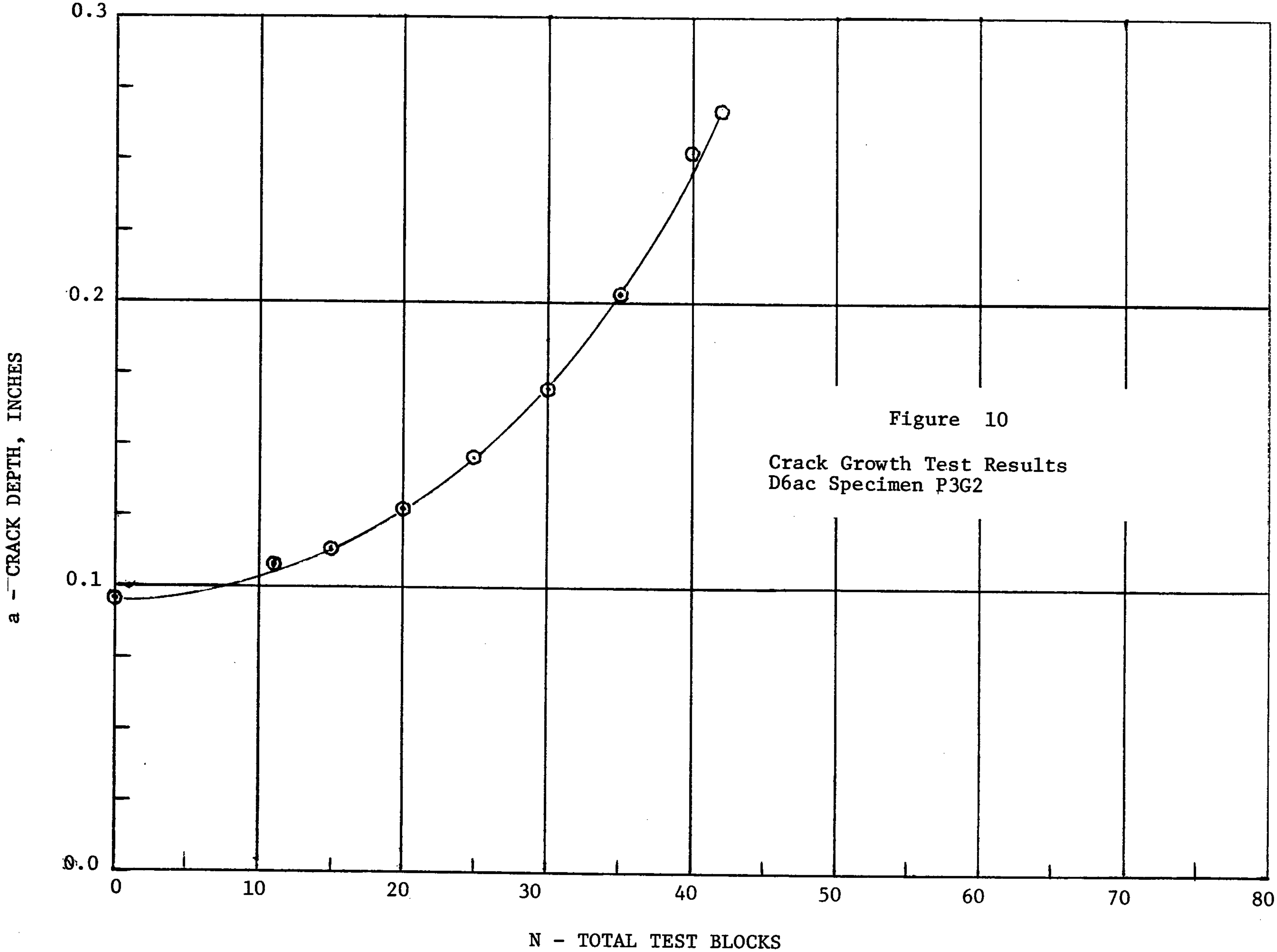

Figure 10

Crack Growth Test Results
D6ac Specimen P3G2

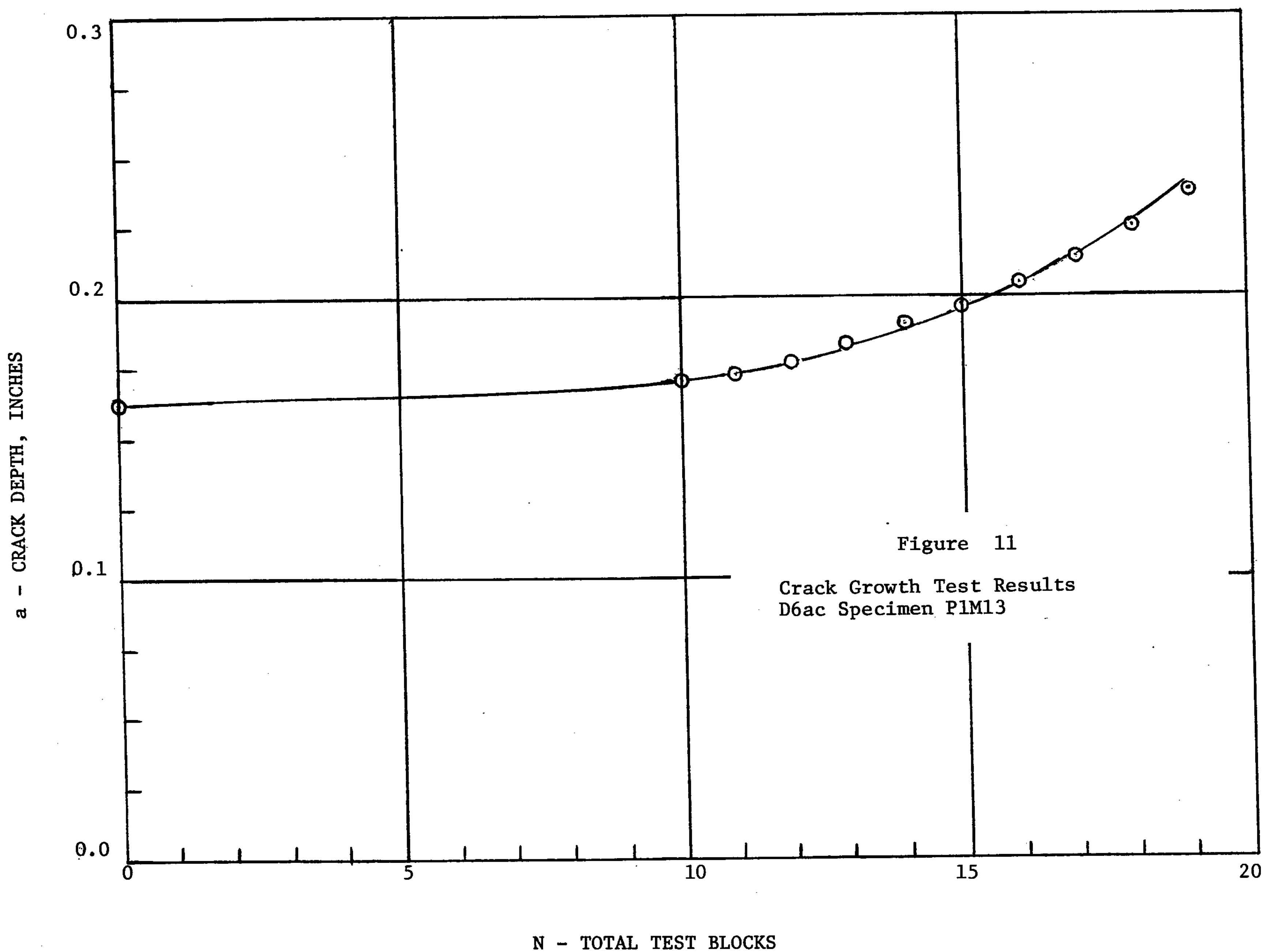

Figure 11

Crack Growth Test Results
D6ac Specimen P1M13

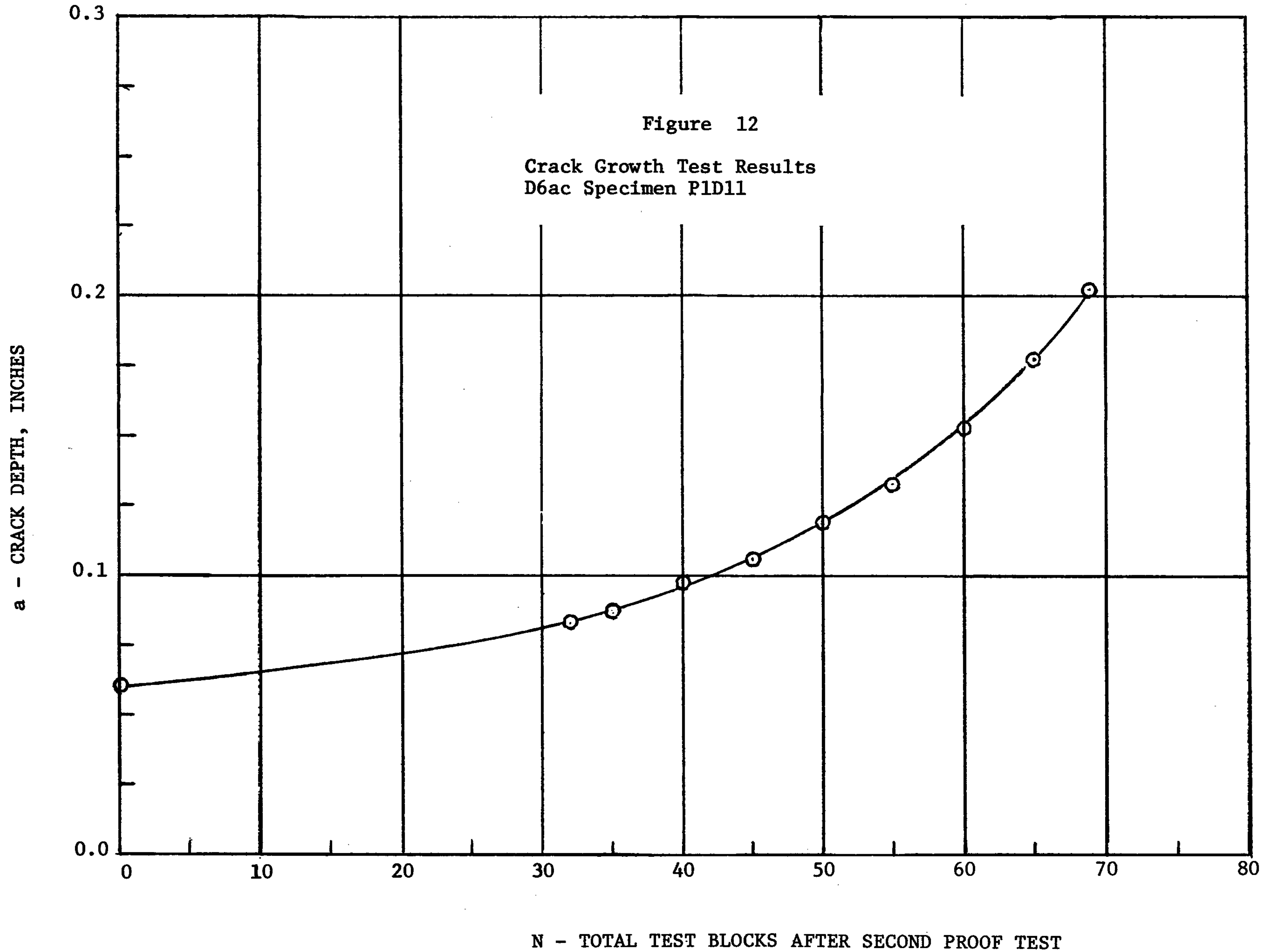

Figure 12

Crack Growth Test Results
D6ac Specimen P1D11

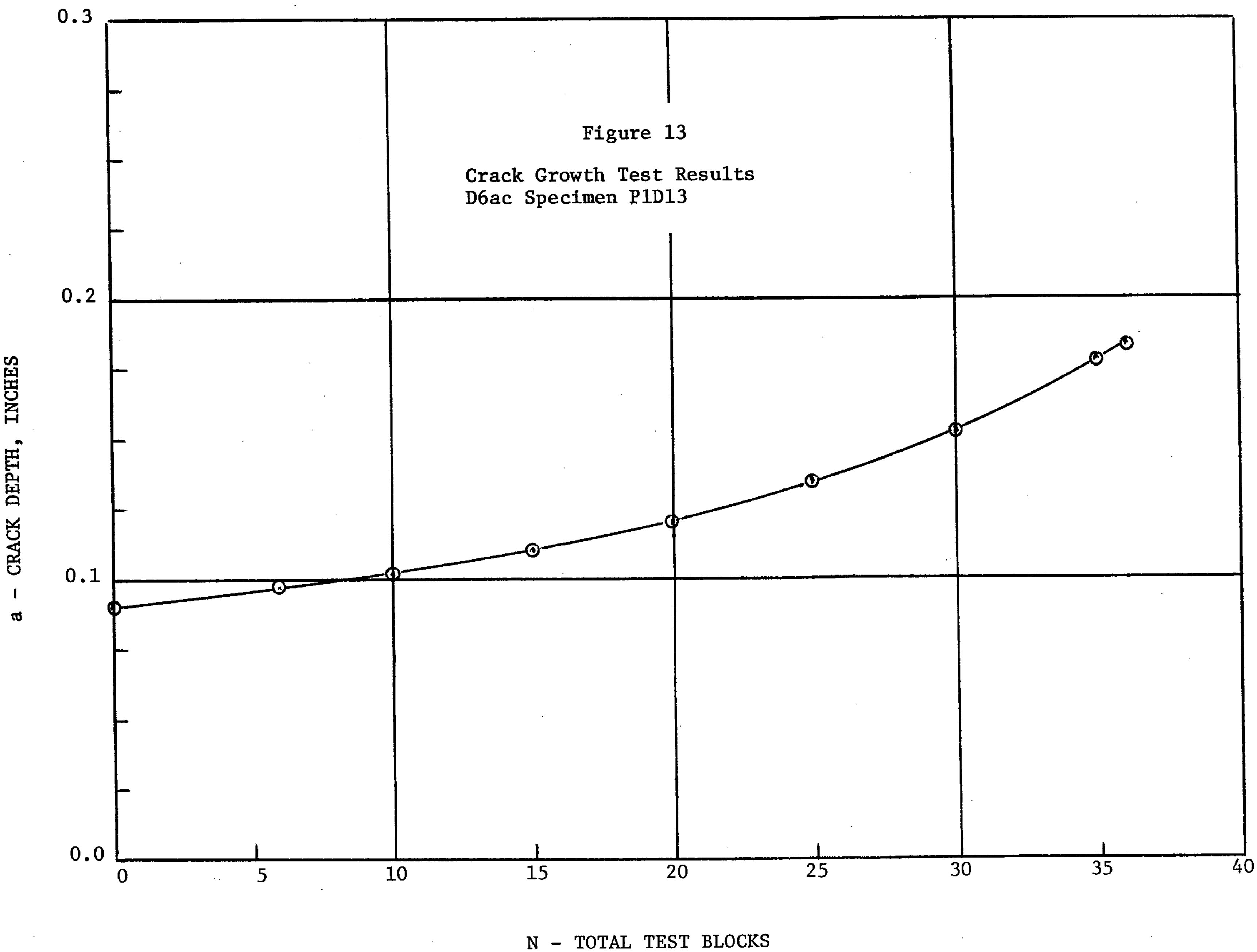

Figure 13

Crack Growth Test Results
D6ac Specimen P1D13

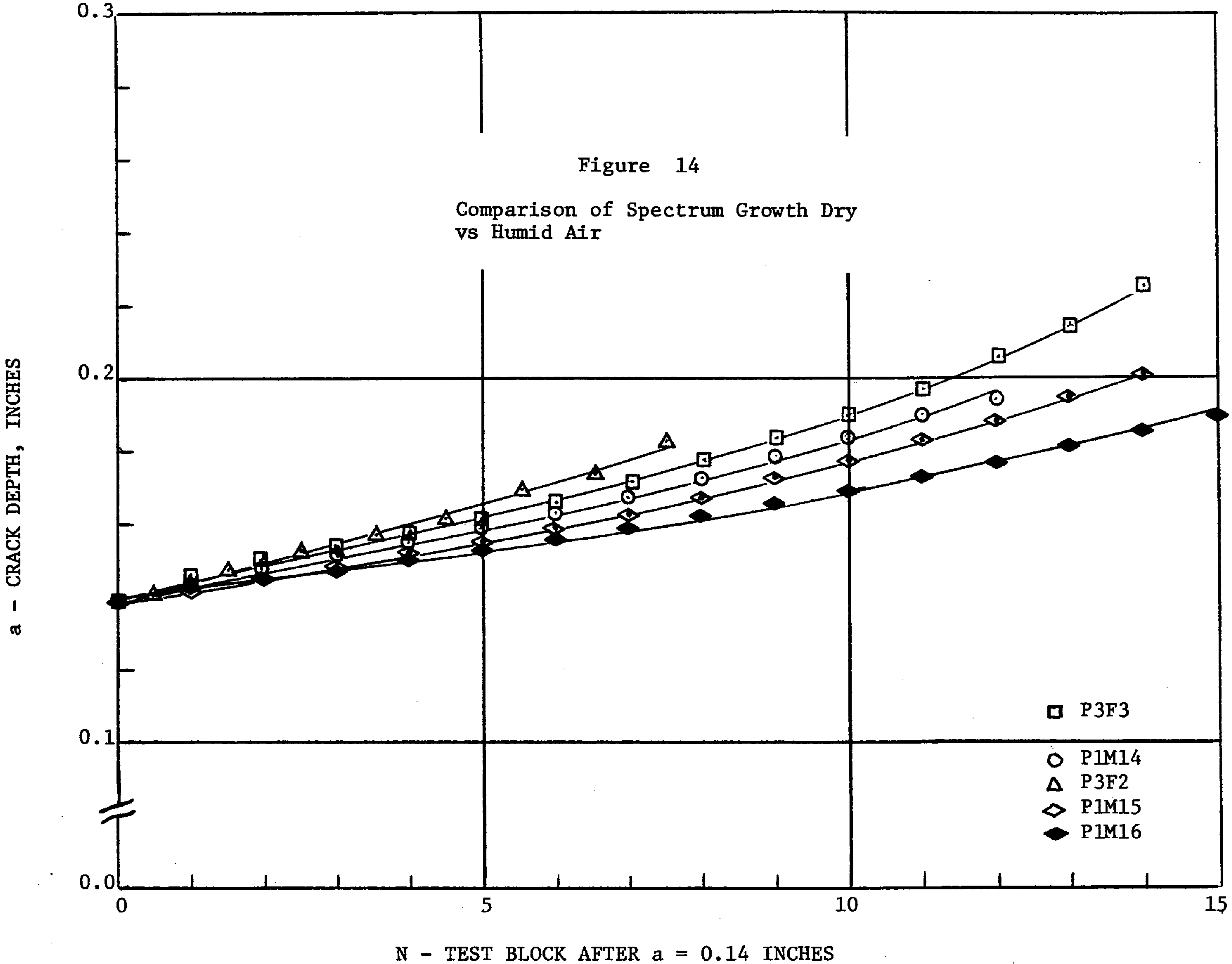

Figure 14

Comparison of Spectrum Growth Dry vs Humid Air

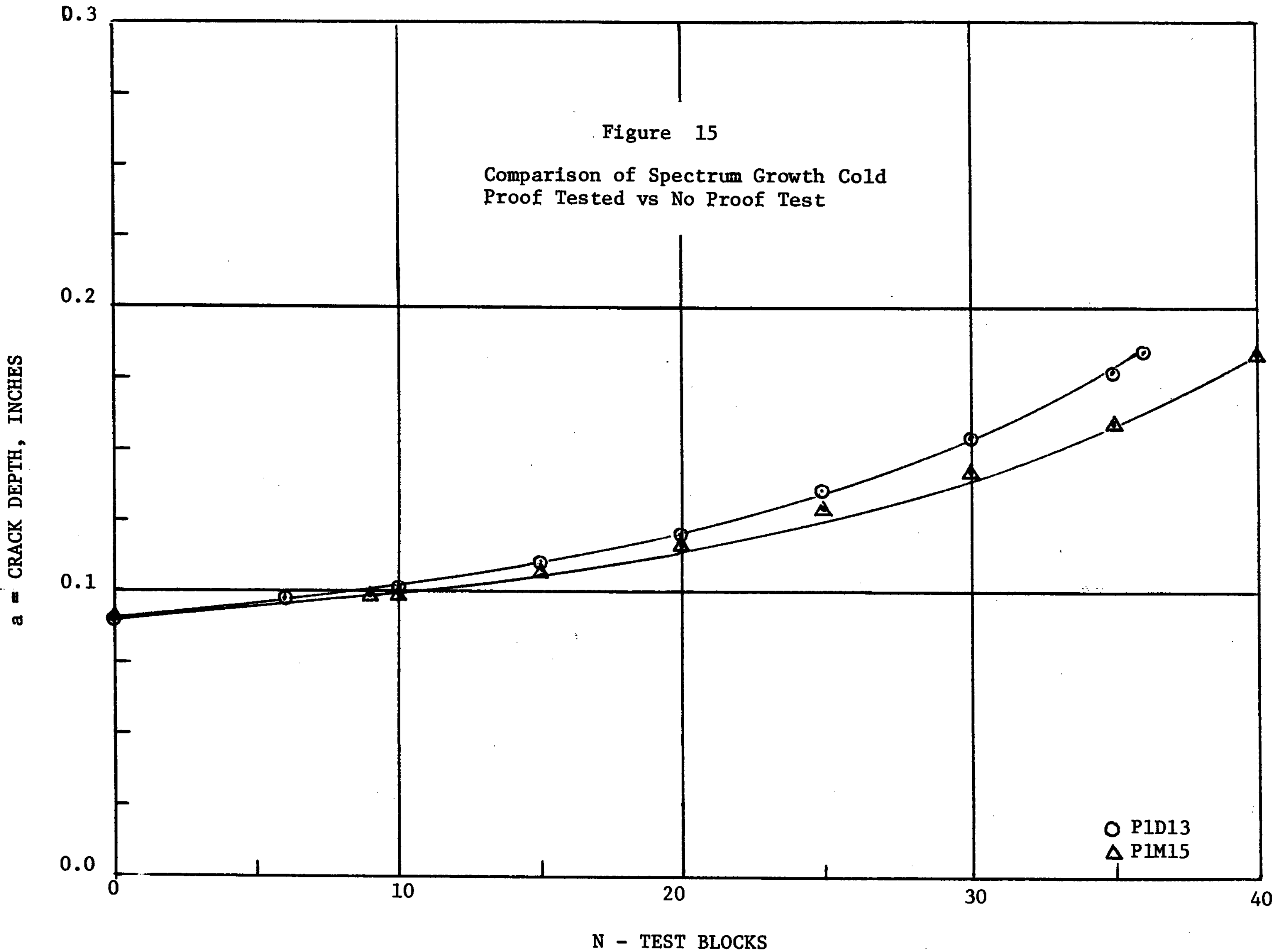

Figure 15

Comparison of Spectrum Growth Cold Proof Tested vs No Proof Test

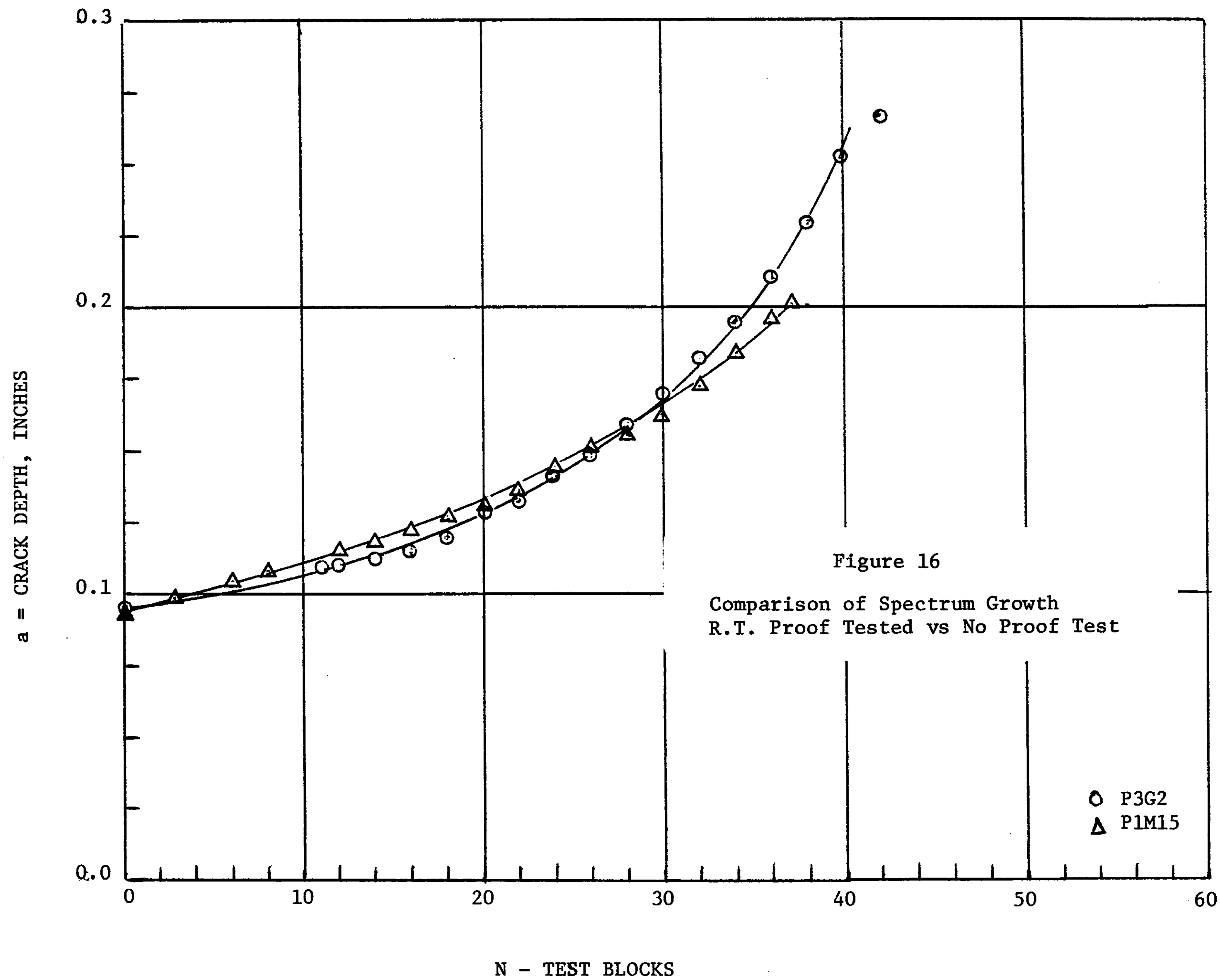

Figure 16

Comparison of Spectrum Growth
R.T. Proof Tested vs No Proof Test

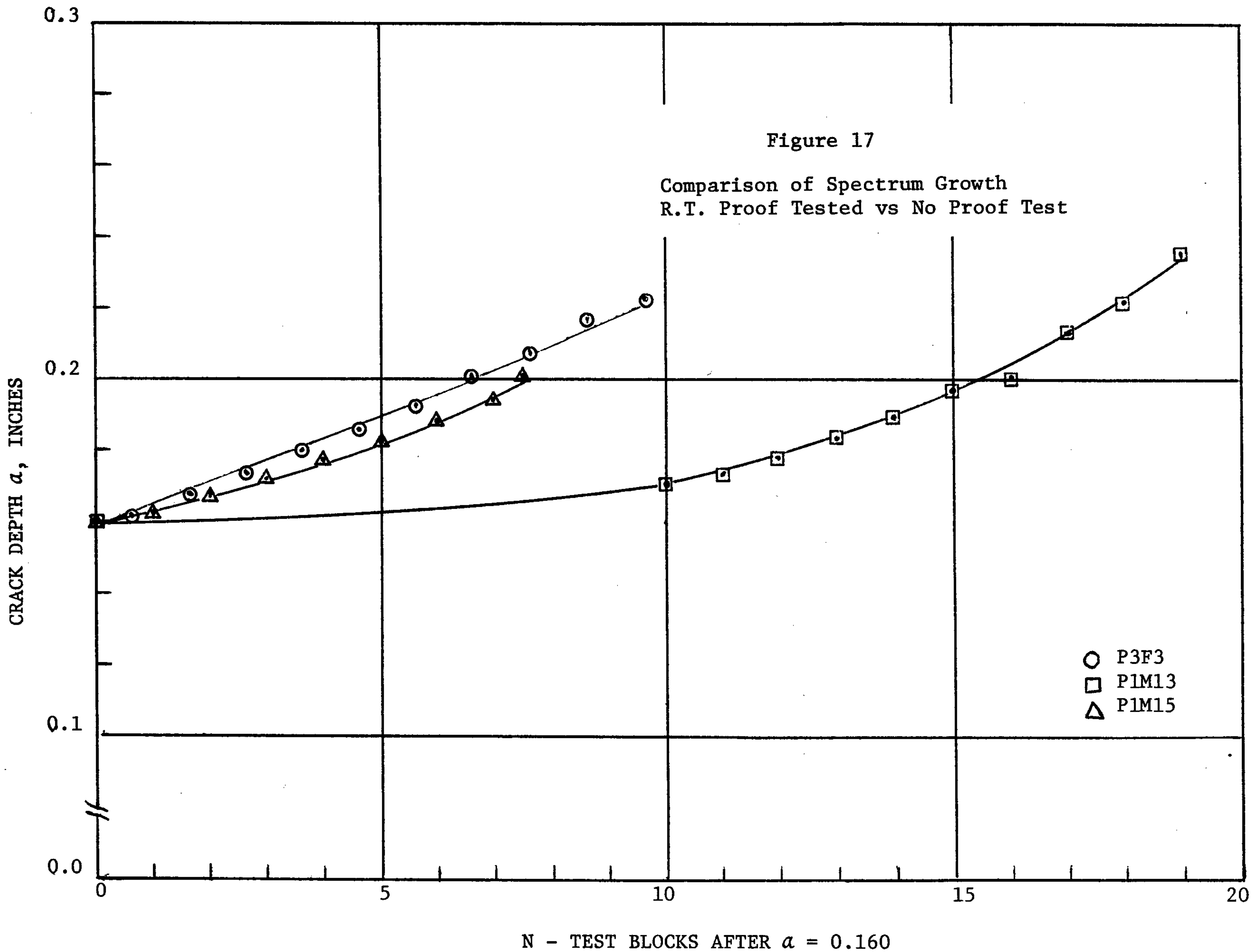

Figure 17

Comparison of Spectrum Growth
R.T. Proof Tested vs No Proof Test

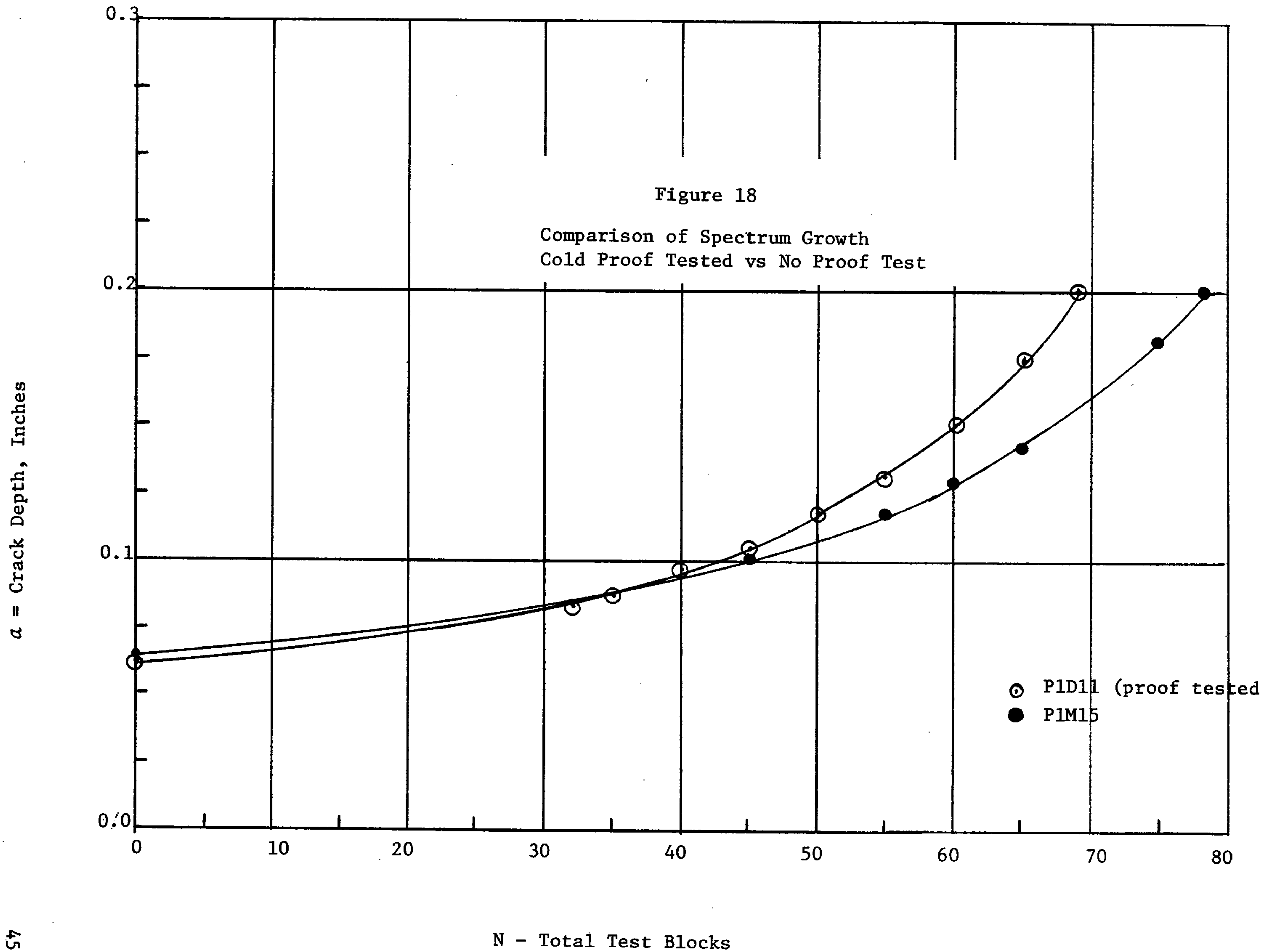

Figure 18

Comparison of Spectrum Growth
Cold Proof Tested vs No Proof Test

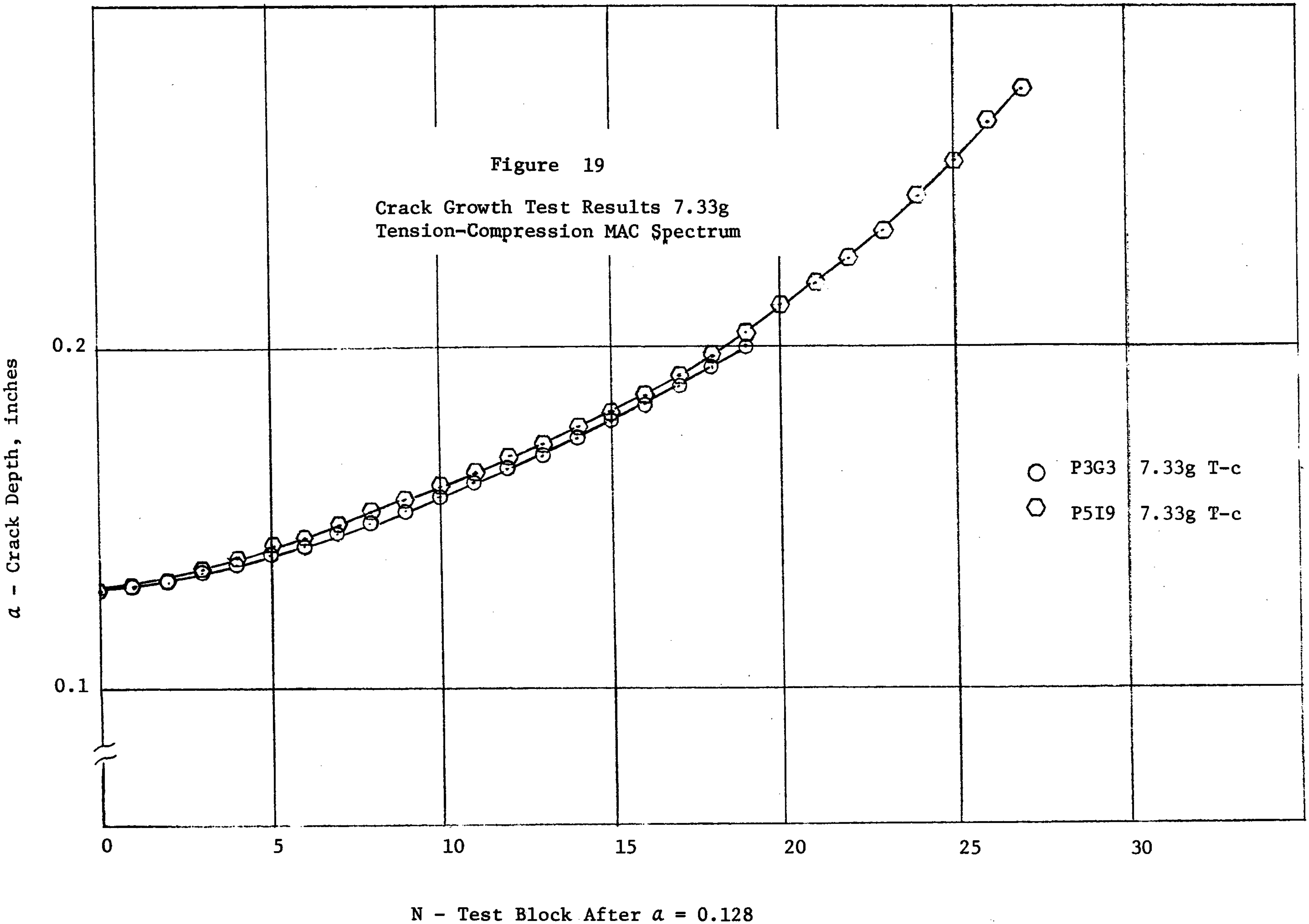

Figure 19

Crack Growth Test Results 7.33g
Tension-Compression MAC Spectrum

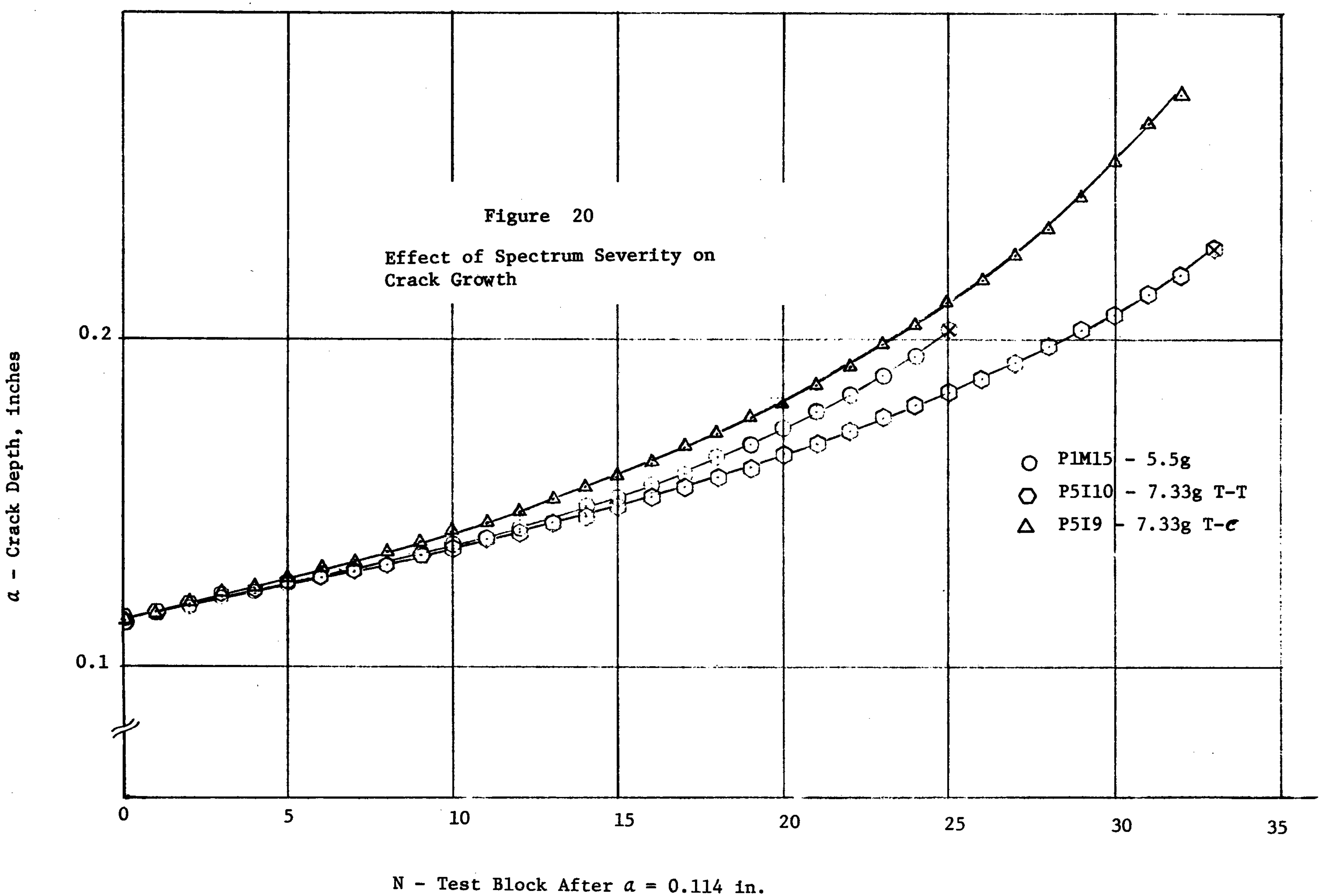

Figure 20

Effect of Spectrum Severity on Crack Growth

V Conclusions

1. Spectrum tests conducted on surface flawed D6ac plate material have indicated relatively long periods of crack growth for randomized block loading.

2. The overall effect of a single proof stress cycle should be the retardation of subsequent crack growth, however, for this program, any such effect was apparently "wiped out" after a few test blocks.

3. Laboratory air had an apparent accelerating effect on crack growth over that of a dry nitrogen environment.

4. The increased levels of maximum stress for the 7.33g spectrum caused an apparent delay in crack growth for the order of loading used in this program.

5. The occurrences of stress reversals (compression) in the 7.33g caused an apparent acceleration of crack growth over the 7.33g Tension-Tension spectrum, however, the growth fell within the band of data for the 5.5g spectrum.

REFERENCES

1. Mil-A-008866A (USAF) used in lieu of Mil-A-8866(ASG), 18 May 1960.

2. Private Communication: J. Collipriest, North American Rockwell Corporation.

3. AFML/DMIC Technical Report, "Results of Mechanical Property Testing of D6ac Steel (F-111 Program)" To Be Published.